Static lattice and electron properties of $MgCO_3$ (magnesite) calculated by *ab initio* periodic Hartree-Fock methods

M. Catti
Dipartimento di Chimica Fisica ed Elettrochimica, Università degli Studi di Milano, via Golgi 19, 20133 Milano, Italy

A. Pavese
*Dipartimento di Scienze Mineralogiche e Petrologiche, Università degli Studi di Torino, via V. Caluso 37, 10125 Torino, Italy**

R. Dovesi
Dipartimento di Chimica Inorganica, Fisica e dei Materiali, Università degli Studi di Torino, via Giuria 5, 10125 Torino, Italy

V. R. Saunders
Daresbury Laboratory, Science and Engineering Research Council, Daresbury, Warrington WA4 4AD, United Kingdom
(Received 8 September 1992; revised manuscript received 11 December 1992)

Calculations of the Hartree-Fock ground-state wave function and total energy of crystalline $MgCO_3$ have been performed using the *ab initio* CRYSTAL program. Contracted Gaussian-type functions have been used to represent 18, 18, and 14 (including *d*) atomic orbitals for Mg, O, and C, respectively. The rhombohedral calcite-type structure has been fully relaxed, determining the equilibrium lattice constants and coordinate of the O atom as a function of volume. The bulk elastic modulus and the C_{33} and $C_{11}+C_{12}$ elastic constants have been calculated. Deviations from experimental data are within 1% for the structural parameters and amount to +6.8% for the bulk modulus. The computed binding energy (including a correction for the electron correlation based on local-density-functional theory) is smaller by 6% than the measured value. Mulliken electron charges are +1.750, −0.986, and +1.207 $|e|$ for Mg, O, and C. Energy bands, density of states, and electron-density maps permit the characterization of chemical bonding within the CO_3 molecular unit and between CO_3 groups and Mg atoms.

INTRODUCTION

The hypersurface of the ground-state energy of a crystalline solid can be evaluated as a function of the lattice geometry and of the atomic positions in the unit cell, as for molecules with respect to bond lengths and angles. A number of physical properties can thus be derived, at least in principle: the equilibrium crystal structure at 0 K, its dependence on volume and pressure (hence the static equation of state), the elastic constants, and some features of the phonon-dispersion curves.

Such calculations have often been attempted by the electron-gas approximation[1–4] or the local-density-functional theory[5–7] and applied to simple systems such as alkali halides, alkaline-earth halides, and oxides. On the other hand, use of the *ab initio* periodic Hartree-Fock (HF) method[8] (computer program CRYSTAL[9]) has allowed one to consider the simpler properties of more complicated solids such as quartz,[10] and to investigate in depth the elastic properties with full structural relaxation in the case of CaF_2 (Ref. 11) and MgF_2 (Ref. 12). The case of divalent metal carbonates with the calcite structure is particularly attractive, in this respect, for a number of reasons. First, they are good examples of three-atom oxysalt systems containing a covalently bonded molecular unit (the CO_3^{2-} anion), which interacts mainly ionically with the metal cations. Thus the presence of different kinds of bonding in the same crystal is an interesting test of the HF method. On the other hand, the rhombohedral calcite-type crystal structure[13] (space group $R\bar{3}c$) has only three independent geometrical parameters, so a detailed study of lattice and electron properties is feasible. Second, there is great interest in ACO_3 carbonates both in the chemistry of raw materials and in the earth sciences,[14] so that much effort has been directed to characterize phase transitions, equation of state, elastic and vibrational properties,[15] and kinetics of chemical reactions of these compounds. In parallel, extensive theoretical work by classical, partly empirical interatomic potential functions has been performed to model the same properties.[16,17] The simplest compound of the series if $MgCO_3$ (magnesite), and has been considered for the present study. A subsequent paper on calcite, $CaCO_3$, is in preparation.[18] The crystal structure of magnesite has been determined by several authors, at various temperatures;[19] in particular, an accurate x-ray study[20] also allowed the construction of experimental maps of electron density. The full set of elastic constants is also available.[21] On the other hand, little theoretical work by quantum methods is available for crystalline $MgCO_3$: we

are aware of a single paper[22] using a mixed approach, i.e., a HF self-consistent-field (SCF) calculation (at the 4-31G level) for the free CO_3^{2-} ion, supplemented by a modified-electron-gas (MEG) approximation to account for Mg^{2+}-CO_3^{2-} interactions in the crystal.

In the present study the periodic HF-SCF method (CRYSTAL program) is applied to the calculation of the equilibrium structural configuration of magnesite versus volume, including a full internal relaxation, and of some of its elastic properties. The chemical bonding is characterized by computing the electron band structure, the density of states and related properties, and some electron-density maps on chemically relevant planes. A separate paper, now in preparation, will deal with calculations of the x-ray structure factors and comparison with experimental values.

COMPUTATIONAL METHOD

The CRYSTAL program,[9] on the all-electron *ab initio* Hartree-Fock linear combination of atomic orbitals formalism applied to periodic systems (crystalline solids, slabs, polymers),[8] was used for all the calculations. Every atomic orbital is expressed as a linear combination of Gaussian-type functions, consisting of a radial Gaussian multiplied by a real solid harmonic function. The basis set utilized for Mg contains 18 atomic orbitals and is denoted as 8-511G* (cf. Ref. 23). Except for the addition of *d*-types orbitals, it corresponds to that adopted in the MgF_2 study.[12] An attempt to optimize the exponent of the outer shell made it drift towards lower values with hardly significant gain of energy, so that the starting value was kept. For the O and C atoms, 18 and 14 orbitals were used, respectively, and the corresponding basis sets are indicated as 8-411G* and 6-21G*. The former comes from a previous study of MgO;[24] however, the exponents of the two outermost shells were fully optimized here by minimization of the $MgCO_3$ total crystal energy. The basis set of Ref. 25 was adopted for carbon, but optimizing the exponent of the outer Gaussian and adding a *d*-type shell. Details of the atomic basis sets used are reported in Table I.

The calculations are affected by errors due to the finite size of the variational basis set. This topic is examined below by discussing the effect of omitting the *d* orbitals from the atomic basis sets on the calculated physical properties.

The computational conditions employed in the CRYSTAL calculations[8] were the following. A value of 10^{-5} $|e|$ was assumed for the overlap and penetration threshold of Coulomb and exchange integrals, while 10^{-8} and 10^{-14} $|e|$ were the pseudo-overlap thresholds for the exchange series. The truncated bipolar expansion was used to approximate bielectronic integrals with very small reciprocal penetration (less than 10^{-14} and 10^{-10} for Coulomb and exchange integrals, respectively). The Brillouin zone was sampled at 27 points for diagonalization of the Fock matrix. An estimate of the residual error introduced by these stringent computational conditions was obtained by removing the bipolar expansion approximation, decreasing the threshold values of Coulomb and exchange integrals to 10^{-6}, and increasing the number of sampled points in the Brillouin zone to 216. The total energy per formula unit decreased by 3×10^{-4} hartrees.

LEAST-ENERGY STRUCTURE AND ELASTIC PROPERTIES

The structure of magnesite (Fig. 1) has three geometrical degrees of freedom; with reference to the triple hexagonal unit cell (containing six formula units of $MgCO_3$), these are the edges *a* and *c*, and the fractional coordinate *x* of the O atom. The corresponding experimental values at room temperature[20] are reported in Table II; extrapo-

TABLE I. Exponents (bohr^{-2}) and contraction coefficients of the Gaussian functions adopted for the present study. The contraction coefficients multiply individually normalized Gaussians. $y[\pm z]$ stands for $y\times10^{\pm z}$.

	Carbon			Oxygen			Magnesium		
Shell		Coefficients			Coefficients			Coefficients	
type	Exponents	*s*	*p,d*	Exponents	*s*	*p,d*	Exponents	*s*	*p,d*
1*s*	3.048[+3]	1.826[−3]		4.0[+3]	1.44[−3]		6.837[+4]	2.226[−4]	
	4.564[+2]	1.406[−2]		1.356[+3]	7.64[−3]		9.699[+3]	1.898[−3]	
	1.037[+2]	6.876[−2]		2.485[+2]	5.37[−2]		2.041[+3]	1.105[−2]	
	2.923[+1]	2.304[−1]		6.953[+1]	1.682[−1]		5.299[+2]	5.006[−2]	
	9.349	4.685[−1]		2.389[+1]	3.604[−1]		1.592[+2]	1.691[−1]	
	3.189	3.628[−1]		9.276	3.861[−1]		5.468[+1]	3.670[−1]	
				3.820	1.471[−1]		2.124[+1]	4.004[−1]	
				1.235	7.105[−2]		8.746	1.499[−1]	
2*sp*	3.665	−3.959[−1]	2.365[−1]	5.219[+1]	−8.73[−3]	9.22[−3]	1.568[+2]	−6.240[−3]	7.72[−3]
	7.705[−1]	1.216	8.606[−1]	1.033[+1]	−8.979[−2]	7.068[−2]	3.103[+1]	−7.882[−2]	6.427[−2]
				3.210	−4.079[−2]	2.043[−1]	9.645	−7.992[−2]	2.104[−1]
				1.235	3.767[−1]	3.496[−1]	3.711	2.906[−1]	3.431[−1]
							1.611	5.716[−1]	3.735[−1]
3*sp*	0.26	1.0	1.0	4.790[−1]	4.225[−1]	2.777[−1]	0.68	1.0	1.0
4*sp*				0.23	1.0	1.0	0.28	1.0	1.0
d	0.8		1.0	0.8		1.0	0.8		1.0

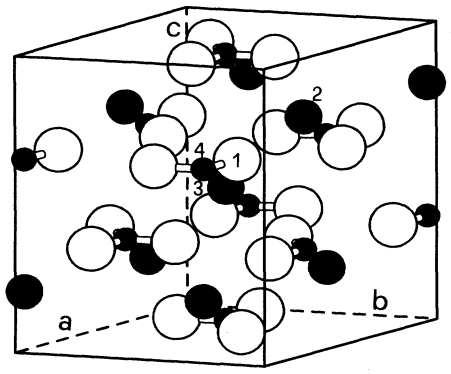

FIG. 1. Hexagonal unit cell of the $MgCO_3$ structure. Black, gray, and open circles represent C, Mg, and O atoms, respectively. The labeled atoms appear in the maps of Figs. 11 and 12.

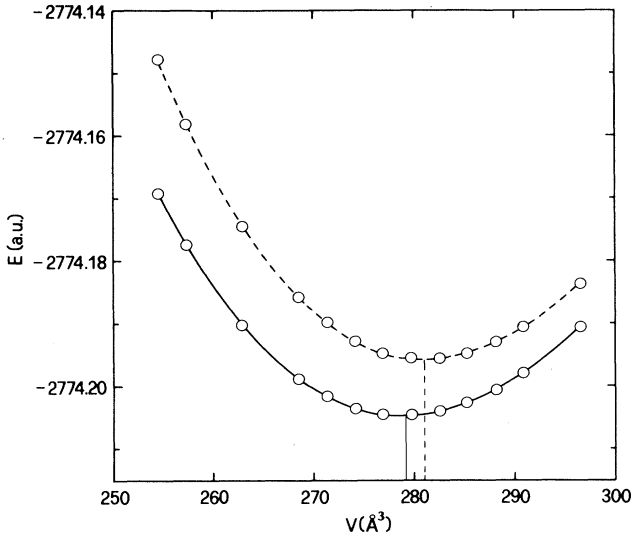

FIG. 2. Energy vs volume curves for the hexagonal unit cell (containing six $MgCO_3$ units). The dashed and full lines correspond to neglecting and including, respectively, the structural relaxation.

lation to 0 K was performed by a parabolic fitting of data measured in the range 300–773 K (Ref. 19). We have preferred to choose three other structural variables related to the previous ones: the volume of the hexagonal unit cell $V=(\sqrt{3}/2)a^2c$, the ratio $q=c/a$ and the C-O bond length $r_{C\text{-}O}=ax$. The total (electronic + nuclear) crystal energy is a function $E(V,q,r_{C\text{-}O})$ of all three variables, but only V is independent, as the least-energy conditions $(\partial E/\partial q)_{V,r}=0$ and $(\partial E/\partial r_{C\text{-}O})_{V,q}=0$ lead to $q=q(V)$ and $r_{C\text{-}O}=r_{C\text{-}O}(V)$ functional dependencies: thus at equilibrium $E=E(V)$. At first the energy was computed keeping q and $r_{C\text{-}O}$ fixed at their experimental values, and changing V in the range -9% to $+6\%$ with respect to the experimental volume: the dashed curve in Fig. 2 (unrelaxed energy) was obtained. Then the q ratio was relaxed for 6 of the 13 V values considered (-9%, -6%, -3%, 0%, $+3\%$, $+6\%$), by computing $E(q,V)$ and finding the optimum $q(V)$ numerically from the minimum energy condition (Table III). With the optimized q values, the $r_{C\text{-}O}$ bond length was relaxed in its turn for $\Delta V/V=-9\%$, -6%, 0%, $+6\%$; the $E(r_{C\text{-}O},V)$ surface was calculated and the best $r_{C\text{-}O}$ lengths were determined by the condition $(\partial E/\partial r_{C\text{-}O})_V=0$, yielding the linear fit (Fig. 3, full line):

$$r_{C\text{-}O}=1.1896+2.8150\times10^{-4}\,V\ .$$

Eventually, the q ratio versus V was optimized again by using the above computed $r_{C\text{-}O}(V)$ distance instead of its fixed experimental value (Table III), and the results were least-squares interpolated according to the following polynomial (Fig. 4, full line):

$$q=13.285\,09-0.117\,918\,V$$
$$+4.474\,99\times10^{-4}\,V^2-5.500\,95\times10^{-7}\,V^3\ .$$

By computing the energy for each volume with the optimized $r_{C\text{-}O}$ and q quantities, instead of the fixed equilibrium experimental values, the $E(V)$ curve for the fully relaxed structure was obtained (Fig. 2, full line). By poly-

TABLE II. Computed (without and with d orbitals on all atoms) vs experimental structural and elastic properties of $MgCO_3$. Relative errors are referred to the $T=0$ K column.

	Expt.		Calc.			
	$T=300$ K[a]	$T=0$ K[b]	no d	$\Delta\%$	d	$\Delta\%$
a (Å)	4.636	4.632	4.648	+0.3	4.617	−0.3
c (Å)	15.026	14.991	14.957	−0.2	15.108	+0.8
x(O)	0.2775	0.2777	0.2768	−0.3	0.2747	−1.1
V (Å^3)	279.7	278.5	279.9	+0.5	278.9	+0.1
$q=c/a$	3.241	3.236	3.218	−0.6	3.273	+1.1
$r_{C\text{-}O}$ (Å)	1.2865	1.2865	1.287	0.0	1.268	−1.4
B (GPa)	110	117	123	+5.1	125	+6.8
C_{33} (GPa)	156	159	186	+17.0	187	+17.6
$C_{11}+C_{12}$ (GPa)	334	361	401	+11.1	392	+8.6

[a]References 20 and 21 for structural and elastic data, respectively.
[b]For structural data, parabolic extrapolations of high-T measurements in Ref. 19. For elastic data, the linear extrapolations assume the same temperature coefficients determined for calcite (Ref. 27).

TABLE III. Computed E (energy of the hexagonal unit cell of $MgCO_3$+2774 hartrees) vs volume (Å^3); the optimization against $q=c/a$ and $r_{C\text{-}O}$ in three steps is reported. For the first E column, $r_{C\text{-}O}=1.2865$ Å; for the second and third ones $q(V)$ and $r_{C\text{-}O}(V)$, respectively, take the values optimized in the previous step.

V	q	E	$r_{C\text{-}O}$	E	q	E
254.51	3.0340	−0.143 35	1.247 90	−0.163 71	3.0740	−0.163 89
	3.0740	−0.146 90	1.254 33	−0.167 52	3.1147	−0.166 95
	3.1147	−0.149 21	1.260 76	−0.168 85	3.1561	−0.168 68
	3.1561	−0.150 06	1.267 19	−0.167 80	3.1983	−0.169 27
	3.1983	−0.149 59	1.273 63	−0.164 07	3.2412	−0.168 31
	3.2412	−0.147 78			3.2848	−0.165 92
	3.2848	−0.144 49			3.3293	−0.162 15
optimum	3.1629	−0.150 09	1.261 02	−0.168 89	3.1918	−0.169 22
262.90	3.0757	−0.169 53	1.250 47	−0.184 72	3.0757	−0.182 19
	3.1160	−0.172 71	1.255 61	−0.187 99	3.1160	−0.186 09
	3.1570	−0.174 60	1.260 76	−0.189 69	3.1570	−0.188 67
	3.1987	−0.175 21	1.265 91	−0.189 80	3.1987	−0.190 02
	3.2412	−0.174 43	1.271 05	−0.188 37	3.2412	−0.189 91
	3.2844	−0.172 17	1.276 20	−0.185 32	3.2844	−0.188 53
	3.3283	−0.168 60			3.3283	−0.185 77
optimum	3.1954	−0.175 20	1.263 73	−0.189 95	3.2184	−0.190 13
271.29	3.0774	−0.181 36			3.1173	−0.195 05
	3.1579	−0.188 13			3.1579	−0.198 54
	3.1991	−0.189 52			3.1991	−0.200 67
	3.2412	−0.189 73			3.2412	−0.201 51
	3.2839	−0.188 63			3.2839	−0.201 04
	3.3274	−0.186 13			3.3274	−0.199 23
	3.4167	−0.176 95			3.3717	−0.196 03
optimum	3.2261	−0.189 83			3.2470	−0.201 54
279.68	3.0020	−0.170 82	1.255 61	−0.199 37	3.1185	−0.195 51
	3.0790	−0.183 69	1.260 76	−0.202 57	3.1587	−0.199 56
	3.1587	−0.191 94	1.265 91	−0.204 14	3.1996	−0.202 38
	3.2412	−0.195 45	1.271 05	−0.204 20	3.2412	−0.204 08
	3.3265	−0.193 75	1.276 20	−0.202 64	3.2835	−0.204 43
	3.4149	−0.186 92	1.281 34	−0.199 80	3.3265	−0.203 49
	3.5065	−0.174 21			3.4149	−0.197 67
optimum	3.2573	−0.195 53	1.268 71	−0.204 35	3.2748	−0.204 45
288.07	3.1595	−0.187 91			3.1595	−0.193 38
	3.2000	−0.191 06			3.2000	−0.196 89
	3.2412	−0.192 91			3.2412	−0.199 20
	3.2835	−0.193 67			3.2835	−0.200 34
	3.3257	−0.193 14			3.3257	−0.200 34
	3.3690	−0.191 22			3.3690	−0.198 95
	3.4131	−0.188 03			3.4580	−0.192 15
optimum	3.2858	−0.193 67			3.3021	−0.200 49
296.46	3.1602	−0.177 31	1.260 76	−0.186 45	3.1602	−0.181 20
	3.2004	−0.181 07	1.265 91	−0.189 18	3.2004	−0.185 27
	3.2412	−0.183 60	1.271 05	−0.190 43	3.2412	−0.188 18
	3.2826	−0.185 03	1.276 20	−0.190 05	3.2826	−0.189 93
	3.3249	−0.185 20	1.281 34	−0.188 34	3.3249	−0.190 55
	3.3678	−0.184 06	1.286 49	−0.185 31	3.3678	−0.189 84
	3.4115	−0.181 92			3.4115	−0.188 03
	3.5011	−0.173 47			3.5011	−0.180 43
optimum	3.3100	−0.185 26	1.2728	−0.190 43	3.3241	−0.190 52

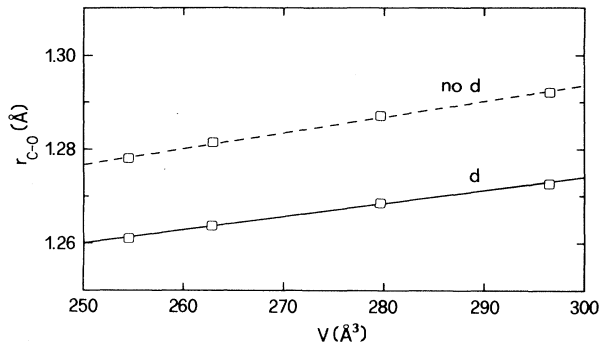

FIG. 3. Optimized C-O bond length vs volume with and without d orbitals.

nomial interpolations, the equilibrium least-energy volume V_0 was derived, and by substitution into the above $q(V)$ and $r_{C\text{-}O}(V)$ relations all other structural parameters were determined and compared to experimental values (Table II). The calculated volume is in excellent agreement with that extrapolated to 0 K from x-ray data; neglecting the structure relaxation, a slightly larger volume (281.1 Å^3) would be obtained (cf. Fig. 2). On the other hand, the equilibrium c/a ratio and $r_{C\text{-}O}$ bond length are somewhat over- and underestimated, respectively, by comparison with measured values.

In order to assess the importance of polarization functions for reproducing the equilibrium geometry, the whole calculation was repeated by omitting the d orbitals from the basis sets of all three atoms Mg, C, and O. In Figs. 3 and 4, the dashed interpolation lines show the obtained dependences of $r_{C\text{-}O}$ and c/a on volume, respectively. The slopes are very similar to results with d orbitals, but the line positions are shifted towards smaller (c/a) and larger ($r_{C\text{-}O}$) values. Thus the equilibrium C-O distance (Table II) reproduces exactly the experimental value, while the unit cell is slightly compressed rather than elongated (as in the d case) along c, with respect to the measured data. It is not surprising that inclusion of d orbitals in the atomic basis sets produces a shortening of the C-O bond length in the CO_3 group, and a slightly

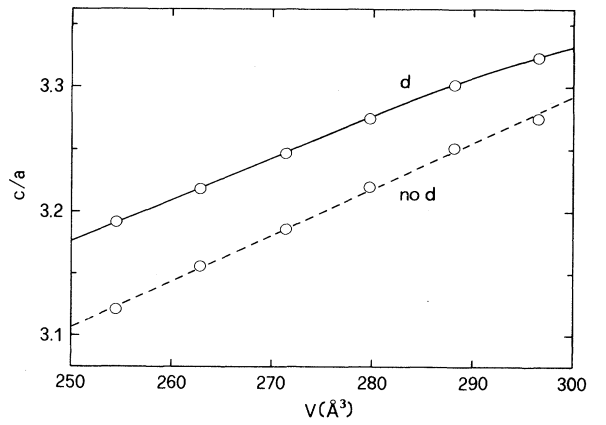

FIG. 4. Optimized ratio of unit-cell edges c/a vs volume, with and without d orbitals in the atomic basis sets.

worse agreement with experimental data, if we consider results of Hartree-Fock calculations on molecular systems.[23] In particular, the C-O distances in CO and H_2CO molecules are computed to be 1.114 and 1.184 Å, respectively, with 6-31G* basis sets, against values of 1.129 and 1.207 Å with 3-21G basis sets and experimental values of 1.128 and 1.208 Å. It is concluded in Ref. 23 that lengths of multiple bonds are consistently underestimated by basis sets including polarization functions, typically by 0.01–0.02 Å. Electron correlation effects are largely responsible, and neglect of d orbitals shows an apparent improvement simply by compensation of opposite errors. These results are fully confirmed in a molecular crystal-like $MgCO_3$.

The dependence of the energy on volume, if interpolated by a suitable analytical formula, yields all relevant information on the equation of state of magnesite at 0 K. The Murnaghan equation,[26] widely used in solid-state thermodynamics, is based on the assumption of a linear dependence of the elastic bulk modulus on pressure ($B=B_0+B'p$):

$$E(V)=B_0V_0\left[\frac{1}{B'(B'-1)}\left(\frac{V_0}{V}\right)^{B'-1}+\frac{1}{B'}\frac{V}{V_0}-\frac{1}{B'-1}\right]+E_0 .$$

By interpolation of the computed $E(V)$ points, the following values were obtained for the Murnaghan parameters: $V_0=279.16$ Å^3, $E_0=-2774.2046$ hartrees, $B_0=124.73$ GPa, $B'=3.08$. By differentiation of the $E(V)$ function, the pressure $p(V)=-dE/dV$ can be obtained, and thus a full representation of the thermodynamical behavior of $MgCO_3$ at 0 K. As experiments are almost always done at constant pressure, rather than at constant volume, it can be useful to transform the computed dependences on volume of structural parameters of $MgCO_3$ into pressure dependences. This was done using the $p(V)$ Murnaghan relation, and the results are shown in Fig. 5 for the unit-cell edges c and a and for the C-O bond length; the very different compressibilities of such distances are evident.

The elastic bulk modulus $B=V_0(d^2E/dV^2)_{V=V_0}$ was computed straightforwardly from the $E(V)$ curve by polynomial interpolations, while of the elasticity tensor only the C_{33} component and the $C_{11}+C_{12}$ linear combination could be calculated in a simple way. The relations used are

$$C_{33}=(1/V_0)c^2(\partial^2E/\partial c^2)_{c=c_0}$$

and

$$C_{11}+C_{12}=(1/2V_0)a^2(\partial^2E/\partial a^2)_{a=a_0} .$$

The deformations involved preserve the full symmetry of the crystal structure. To derive other elastic constants, the symmetry must be lowered with a consequent need of complex calculations for structural relaxation. For the present deformations only the $r_{C\text{-}O}(V)$ relaxation need by

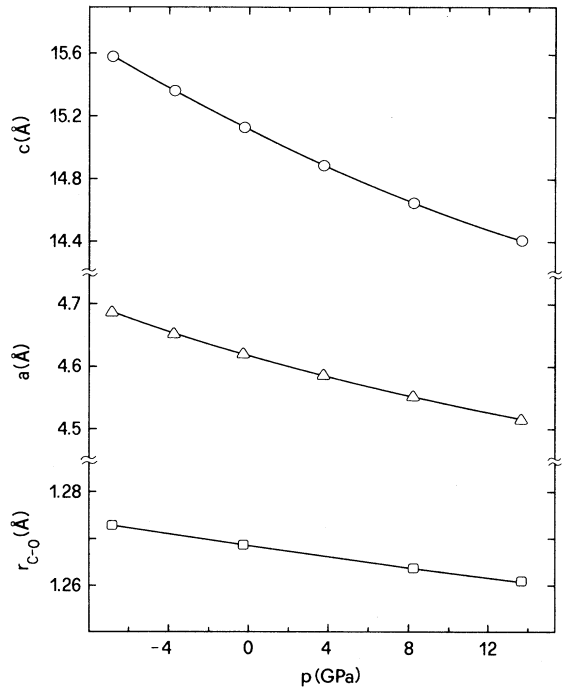

FIG. 5. Computed dependence on pressure of the unit-cell edges and of the C-O bond length of magnesite.

considered. The results are reported in Table II. The effect of *d* orbitals on the computed elastic properties seems to be small, except perhaps for the $C_{11}+C_{12}$ case where some improvement is brought about by use of polarization functions. All calculated values are overestimated with respect to experimental data, and the effect is larger for the C_{33} constant. However, this comparison might not be fully reliable because the data measured at room temperature were extrapolated linearly to 0 K using the temperature dependence of elastic data of calcite,[27] owing to the lack of corresponding results for magnesite. It is also interesting to consider how the elastic properties are affected by the structural relaxation: in the case of B, a value of 139 GPa was obtained from the unrelaxed $E(V)$ curve (dashed line in Fig. 2), instead of 125 GPa. Similar increases are observed also for the elastic constants, if relaxation is neglected.

BINDING ENERGY

The difference between total crystal energy per formula unit (computed for the optimized equilibrium structure) and energies of isolated atoms yielded BE(HF), the Hartree-Fock approximation to the binding energy of $MgCO_3$ (Table IV). The atomic energies were calculated with the basis sets of Table I, omitting the *d* orbitals and adding two diffuse *sp* shells for Mg (8-51111G), and a single shell for O (8-4111G) and for C (6-211G). In this way the more diffuse character of atomic wave functions in the absence of chemical bonds was accounted for. The exponents ($bohr^{-2}$) of the outer shells were optimized, giving values of 0.073 and 0.023 for Mg, 0.487, 0.202, and 0.087 for O, and 0.108 for C. The contribution of electron correlation to the binding energy was estimated by two different density-functional formulas,[28,29] applied to the Hartree-Fock charge densities of the crystal and of the isolated atoms. The δE_1 and δE_2 values (Table IV) are the differences between crystal and atomic correlation energies for the two formulas, respectively.

For a comparison, the experimental value of the binding energy was computed from the formation enthalpy of magnesite at 298 K, by applying a conventional Born-Haber thermochemical cycle. Solid Mg, C, and $MgCO_3$ and gaseous O_2 were ideally cooled down to 0 K; sublimation of Mg and C and dissociation of O_2 molecules followed. Because no heat capacity data could be found for $MgCO_3$, its cooling energy was estimated from the corresponding result of calcite $CaCO_3$. The zero-point

TABLE IV. HF total energy at equilibrium (per $MgCO_3$ unit formula), atomic energies, and binding energy (BE) (hartree). δE_1 and δE_2 are correlation contributions to BE calculated by using charge-density functionals DF_1 (Ref. 28) and DF_2 (Ref. 29), respectively. Δ (%) is the percentage error with respect to BE (expt.).

	$MgCO_3$	Mg	O	C
E(HF)	−462.367 43	−199.604 24	−74.794 27	−37.664 85
BE(HF)	−0.716			
Δ (%)	+31.0			
		Correlation contributions		
DF_1	−1.668	−0.464	−0.261	−0.161
δE_1	−0.260			
BE(HF+DF)	−0.976			
Δ (%)	+6.0			
DF_2	−1.615	−0.448	−0.255	−0.158
δE_2	−0.244			
BE(HF+DF)	−0.960			
Δ (%)	+7.5			
BE (expt.)	−1.038			

vibrational energy of magnesite was evaluated by the Debye model, using a value $\Theta_D = 739$ K obtained by application of Anderson's method[30] to the elastic constants.[21] All other data involved are taken from Ref. 31.

The HF theory substantially underestimates the binding energy (in absolute value), as expected. It should be noticed that omitting the *d* orbitals from the atomic basis sets in $MgCO_3$ would give BE(HF) $= -0.623$ hartree, thus increasing the error to 40%. On the other hand, we believe that the value reported in Table IV is close to the true HF limit. A large improvement is observed by including the correction for electron correlation, and results based on the older density-functional formula[28] seem little different than those based on the more recent one.[29] The residual error may be partly related to the approximations in the correlation correction, partly to some residual inadequacy of the HF variational basis set, and partly to approximations in the thermochemical data used to obtain the experimental binding energy.

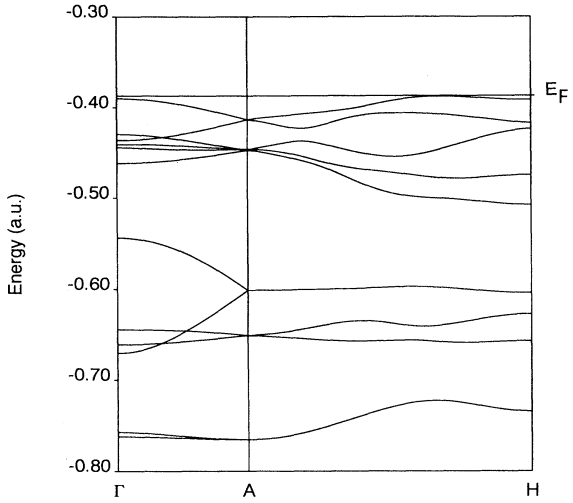

FIG. 6. Structure of the upper set of electron valence bands along two symmetry lines in the first Brillouin zone.

ENERGY BANDS AND CHEMICAL BONDING

A first-approximation overview of electron transfer in magnesite is given by the results of a conventional Mulliken population analysis (Table V). Significant contributions are observed from the *d* shells of all three atoms, but that of C is an order of magnitude larger than the other ones. This confirms the importance of *d* orbitals for a correct account of the C-O bonding. The net atomic charges indicate not only a strong back-transfer of electrons in the covalent C-O bond (consistently with the large overlap population), but also a substantial deviation from ionicity for the Mg-O interaction. The Mg charge is lower than that computed in MgO (1.95 $|e|$),[24] and also in MgF_2 (1.80 $|e|$),[12] with similar orbital basis sets. The Mg-O overlap appears to be populated by a small but significant fraction of electrons, again pointing to the partially covalent bonding between Mg and the carbonate ions. Also noticed should be the relevant antibonding population of the O-O interaction, due to strong repulsion between oxygen atoms belonging to the same CO_3 group.

The charge distribution within the CO_3^{2-} molecular ion can be compared to results obtained for calcite $CaCO_3$ by fitting a point-charge model to structural, elastic, and vibrational experimental data.[16] A potential-energy function consisting of a Born-Mayer two-body term (with $z_{Ca} = 2$ $|e|$, z_O variable, and z_C constrained by electroneutrality) plus a three-body harmonic angular O-C-O term was used. The optimized charges were $z_O = -0.995$ and $z_C = 0.985$ $|e|$ for a rigid-ion model, and $z_O = -1.095$ and $z_C = 1.285$ $|e|$ for a shell model. The agreement with the present results is striking, suggesting a sound physical basis for the point-charge approximation in ionic-molecular solids.

The electron band structure was calculated along the threefold and one of the twofold axes in the first Brillouin zone (Γ-*A* and *A*-*H* lines, respectively). In Fig. 6 a portion corresponding to the upper set of valence bands, just below the Fermi energy, is shown. The high-order degeneracy at the *A* point, and the partial removing of degen-

TABLE V. Mulliken charges and bond populations ($|e|$ units) for individual atoms and for atomic pair overlap in $MgCO_3$.

	Mg	O	C
1*s*	2.000	1.997	1.997
2*sp*	6.456	2.704	1.671
3*sp*	1.448	2.471	0.944
4*sp*	0.327	1.791	
d	0.019	0.023	0.180
total	10.250	8.986	4.793
net charge *z*	+1.750	−0.986	+1.207
	Mg-O	**O-O**	**C-O**
total	+0.029	−0.065	+0.389

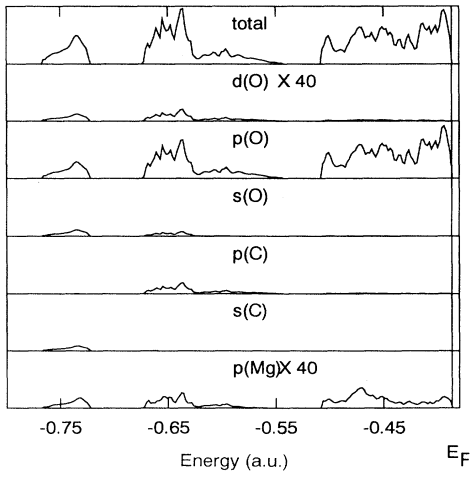

FIG. 7. Total and projected densities of states (DOS) of $MgCO_3$. A Mulliken partition scheme was used to obtain atomic orbital contributions.

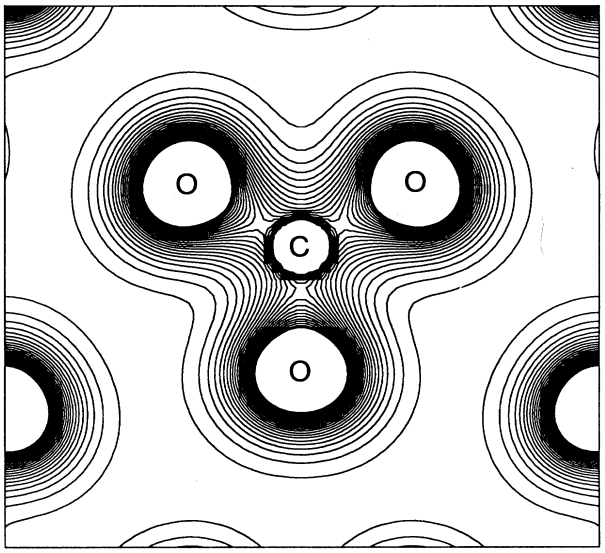

FIG. 8. Total electron-density map on the plane of the CO_3 molecular unit. Contour lines are separated by 0.025 e bohr^{-3}.

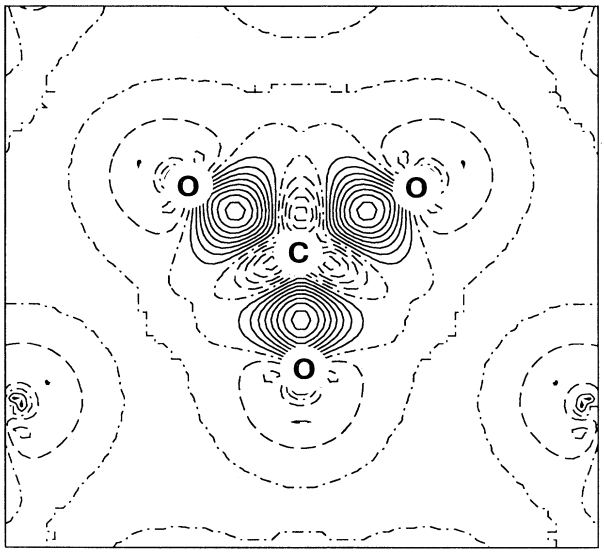

FIG. 10. Difference map between the electron densities computed with and without d orbitals, on the plane of the CO_3 group. Symbols and scale as in Fig. 9.

eracy along the Γ-A with respect to the A-H path appears clearly. The computed energy gap amounts to 0.64 hartree; this value should be a substantial overestimate, as usual for Hartree-Fock calculations, but is consistent with the insulating nature of the $MgCO_3$ crystal. A more complete picture of the electron energy distribution is given by the density of states (DOS), reported in Fig. 7 for the same energy range considered in Fig. 6. In particular, by projecting the total DOS onto contributions of specific atomic orbitals, it is possible to interpret the band structure of valence electrons. All three upper bands, starting from the Fermi energy downwards, are contributed by the p orbitals of O, plus s(O) and p(C) in the second band and s(O) and s(C) in the third one. Thus the first band is related to excess p electrons on O giving rise to the mainly ionic interaction with Mg. The second band, on the other hand, and to a lesser extent the third one as well, correspond to sp overlap in the C-O covalent bonding. This finely structured DOS of magnesite should be compared to the much simpler ones found for MgO and MgF_2, where the upper valence band gives a single sharp peak due to p(O) or p(F) electrons only.

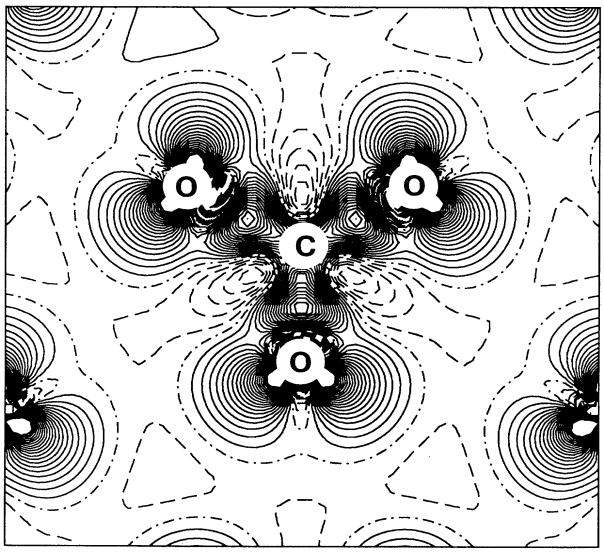

FIG. 9. Difference (crystal minus atomic superposition) electron-density map on the plane of the CO_3 molecular unit. Continuous, dashed-dotted, and dashed lines indicate positive, zero, and negative values, respectively. Isodensity curves are separated by 0.005 e bohr^{-3}.

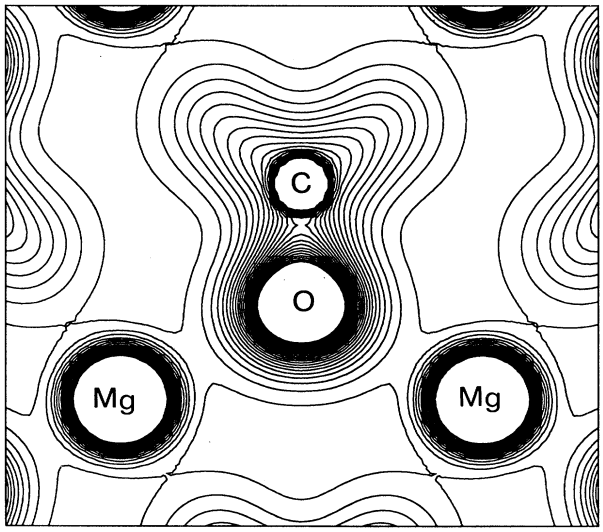

FIG. 11. Total electron density map on the plane 1-2-3-4 in Fig. 1, showing the coordination environment of the O atom. The separation between isodensity curves is 0.025 e bohr^{-3}.

ELECTRON CHARGE DENSITY

The steric and anisotropic character of chemical bonding in magnesite is well represented by maps of total and difference (between crystal and atomic superposition) electron density. Results of this computation on the plane of the CO_3 group are shown in Figs. 8 and 9. The deformation of O atoms from spherical shape can be noticed even in the total map, but is very evident from the difference density. Three main features appear in Fig. 9: the buildup of bonding electron density along the C-O directions, the peculiar two-lobe shape of charge distribution around the O atoms, and the withdrawal of electrons from the angular sectors between C-O directions. These results are fully confirmed by inspection of the deformation density map[20] computed as the difference between experimental x-ray data and data calculated by spherical atomic scattering factors. Similar features are also observed in a difference density map computed for the isolated CO_3^{2-} ion,[22] starting from 4-31G basis sets. Thus the two-lobe shape of the extra electron charge on the oxygen atoms should not be ascribed to intermolecular interactions in the crystal, but rather to the bonding pattern of the carbonate ion. In Fig. 10, a picture is shown of the effect of *d* orbitals on the charge density of the CO_3 group. They appear to contribute substantially to the C-O covalent bonding density, thus giving rise to C-O bond shortening. Also, the electron cloud around the whole carbonate ion contracts significantly, explaining the decrease of intermolecular repulsion and shortening of the *a* cell edge, as discussed above.

Charge-density maps (Figs. 11 and 12) were also calculated on the plane determined by atoms 1, 2, and 3 in Fig. 1, in order to show bonding features in the coordination shell of the O atom. The latter is ionically bonded to two Mg atoms, and attains, with the covalent C-O bond, a planar triangular coordination. The total map (Fig. 11) shows a small but significant electron-density buildup along the Mg-O direction, indicating a covalent contribution to the bonding, consistently with the Mulliken population analysis discussed above.

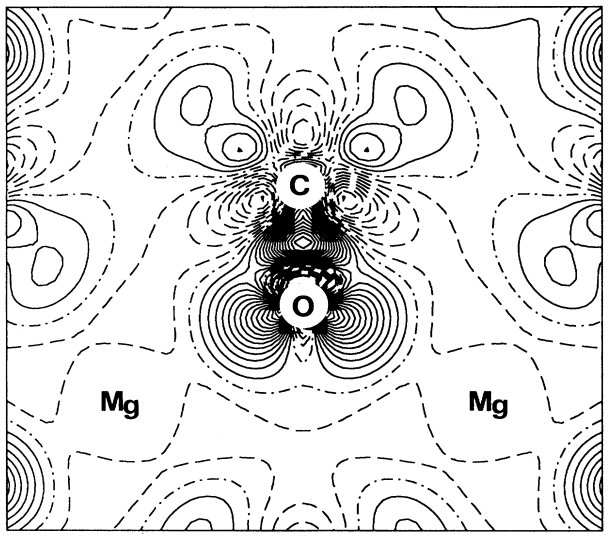

FIG. 12. Difference electron-density map (crystal minus atomic superposition) on the same plane as Fig. 11. Symbols and scale as in Fig. 9.

CONCLUSIONS

A first example of a crystalline solid with the rhombohedral calcite structure, magnesite $MgCO_3$, has been studied by *ab initio* Hartree-Fock techniques. The covalent bonding inside CO_3 molecular units and the prevalently ionic Mg-O interaction have been fully characterized: a non-negligible electron transfer between Mg^{2+} and CO_3^{2-} ions, reflecting partial covalency between these two entities, appears. A detailed picture of structural relaxation as a function of volume has been established, in very good agreement with experimental data at room pressure. These results, together with the evaluation of some relevant elastic properties, allow the prediction of the static equation of state at the athermal limit from first-principles quantum calculations for a ternary solid of significant chemical and structural complexity.

ACKNOWLEDGMENTS

Financial support by the Ministero Univesità e Ricerca Scientifica e Tecnologica (Roma) and by Consorzio per il Sistema Informativo Piemonte (Torino) is gratefully acknowledged.

*Present address: Dipartimento di Scienze della Terra (Sezione di Mineralogia), Università degli Studi di Milano, via Botticelli 23, 20133 Milano, Italy.

[1]C. Muhlhausen and R. Gordon, Phys. Rev. B **23**, 900 (1981).
[2]R. J. Hemley, M. D. Jackson, and R. G. Gordon, Geophys. Res. Lett. **12**, 247 (1985).
[3]R. E. Cohen, L. L. Boyer, and M. J. Mehl, Phys. Rev. B **35**, 5749 (1987).
[4]J. L. Feldman, M. J. Mehl, L. L. Boyer, and N. C. Chen, Phys. Rev. B **37**, 4784 (1988).
[5]J. S. Melvin and D. C. Hendry, J. Phys. C **15**, 2093 (1982).
[6]N. E. Christensen, Phys. Rev. B **33**, 5096 (1986).
[7]M. J. Mehl, R. E. Cohen, and H. Krakauer, J. Geophys. Res. **93**, 8009 (1988).
[8]C. Pisani, R. Dovesi, and C. Roetti, *Hartree-Fock Ab Initio Treatment of Crystalline Solids,* Lecture Notes in Chemistry Vol. 48 (Springer-Verlag, Berlin, 1988).
[9]R. Dovesi, C. Pisani, C. Roetti, M. Causà, and V. R. Saunders, CRYSTAL88. Program No. 577, Quantum Chemistry Program Exchange, Indiana University, Bloomington, IN, 1989.
[10]R. Nada, C. R. A. Catlow, R. Dovesi, and C. Pisani, Phys. Chem. Minerals **17**, 353 (1990).
[11]M. Catti, R. Dovesi, A. Pavese, and V. R. Saunders, J. Phys. Condens. Matter **3**, 4151 (1991).

[12]M. Catti, A. Pavese, R. Dovesi, C. Roetti, and M. Causà, Phys. Rev. B **44**, 3509 (1991).
[13]R. W. G. Wyckoff, Crystal Structures, 2nd ed. (Interscience, New York, 1964), Vol. 2.
[14]J. R. Goldsmith, in *Carbonates: Mineralogy and Chemistry,* Reviews in Mineralogy Vol. 11, edited by R. J. Reeder (Mineralogical Society of America, Washington, DC, 1983), pp. 49–76.
[15]A. Yamamoto, Y. Shiro, and H. Murata, Bull. Chem. Soc. Jpn. **47**, 265 (1974).
[16]A. Pavese, M. Catti, G. D. Price, and R. A. Jackson, Phys. Chem. Minerals, **19**, 80 (1992).
[17]M. Catti, A. Pavese, and G. D. Price, Phys. Chem. Minerals **19**, 472 (1993).
[18]M. Catti, A. Pavese, E. Aprà, and C. Roetti (unpublished).
[19]S. A. Markgraf and R. J. Reeder, Am. Mineral. **70**, 590 (1985).
[20]S. Goettlicher and A. Vegas, Acta Crystallogr. Sect. B **44**, 362 (1988).
[21]M. M. P. Humbert and F. Plicque, C. R. Acad. Sci. Paris Ser. B **275**, 391 (1972).
[22]J. A. Tossel, Physica **131B**, 283 (1985).
[23]W. H. Here, L. Radom, P. R. Schleyer, and J. A. Pople, *Ab Initio Molecular Orbital Theory* (Wiley, New York, 1986).
[24]M. Causà, R. Dovesi, C. Pisani, and C. Roetti, Phys. Rev. B **33**, 1308 (1986).
[25]J. S. Binkley, J. A. Pople, and W. J. Hehre, J. Am. Chem. Soc. **102**, 939 (1980).
[26]F. D. Murnaghan, Proc. Natl. Acad. Sci. U.S.A. **30**, 244 (1944).
[27]D. P. Dandekar and A. L. Ruoff, J. Appl. Phys. **39**, 6004 (1968).
[28]J. P. Perdew, Phys. Rev. B **33**, 8822 (1986).
[29]J. P. Perdew, in *Electronic Structure of Solids,* edited by P. Ziesche and H. Eschrig (Akademie Verlag, Berlin, 1991).
[30]O. L. Anderson, J. Phys. Chem. Solids **24**, 909 (1963).
[31]*Handbook of Chemistry and Physics,* edited by R. C. Weast (Chemical Rubber, Boca Raton, FL, 1987).